

Off-Center Carbon Ignition in Rapidly Rotating, Accreting Carbon-Oxygen White Dwarfs

Hideyuki Saio

Astronomical Institute, Graduate School of Science, Tohoku University, Sendai, 980-8578, Japan

sai0@astr.tohoku.ac.jp

and

Ken'ich Nomoto

Department of Astronomy, Graduate School of Science, University of Tokyo, Hongo 7-3-1, Bunkyo-ku, Tokyo 113-0033, Japan

nomoto@astron.s.u-tokyo.ac.jp

ABSTRACT

We study the effect of stellar rotation on the carbon ignition in a carbon-oxygen white dwarf accreting CO-rich matter. Including the effect of the centrifugal force of rotation, we have calculated evolutionary models up to the carbon ignition for various accretion rates. The rotation velocity at the stellar surface is set to be the Keplerian velocity. The angular velocity in the stellar interior has been determined by taking into account the transport of angular momentum due to turbulent viscosity. We have found that an off-center carbon ignition occurs even when the effect of stellar rotation is included if the accretion rate is sufficiently high; the critical accretion rate for the off-center ignition is hardly changed by the effect of rotation. Rotation, however, delays the ignition; i.e., the mass coordinate of the ignition layer and the total mass at the ignition are larger than those for the corresponding no-rotating model. The result confirms our previous conclusion that a double-white dwarf merger *cannot* be a progenitor of a SN Ia.

Subject headings: accretion – stars: evolution – stars: rotation – supernovae: general – white dwarfs

1. Introduction

Mass accretion onto a white dwarf, which may occur in a close binary system, plays an important role in its evolution. If the accretion rate is sufficiently high, heating of the outer layers of the accreting star leads to the ignition of nuclear burning. A C-O white dwarf accretes C-O rich matter if the companion is also a C-O white dwarf (i.e., double C-O white dwarf system). Whether the carbon is ignited in the stellar center or in the envelope of an accreting C-O white dwarf is crucial for the star's fate. If the ignition occurs at the center, it leads to a SN Ia explosion. If carbon burning is ignited in the envelope, on the other hand, the flame propagates inward to the center

converting the C-O white dwarf to an O-Ne-Mg white dwarf (Saio & Nomoto 1985, 1998; Timmes et al. 1994) that is expected to eventually collapse to a neutron star (Nomoto 1984, 1987; Nomoto & Kondo 1991). Nomoto & Iben (1985) and Kawai et al. (1987) have shown that carbon-ignition occurs in an outer layer if the C-O white dwarf accretes matter more rapidly than $2.7 \times 10^{-6} M_{\odot} \text{y}^{-1}$.

When a double C-O white-dwarf system coalesces due to angular momentum loss by gravitational wave radiation and/or by a magnetic field, the less massive white dwarf is disrupted to become a thick disk around the more massive white dwarf (Iben & Tutukov 1984; Webbink 1984; Benz et al. 1990; Rasio & Shapiro 1995). If the thick disk is turbulent, which is likely, the timescale of

viscous angular momentum transport is very short (Mochkovitch & Livio 1990) so that the more massive white dwarf is expected to accrete CO-rich matter at a rate close to the Eddington limit from the thick disk. Therefore, when a double C-O white-dwarf system coalesces, carbon burning is ignited in the envelope of the more massive white dwarf to transform it to an O-Ne-Mg white dwarf, thus preventing the occurrence of a SN Ia explosion postulated by Iben & Tutukov (1984) and Webbink (1984). In the previous investigations on the carbon ignition, however, the effect of rotation was neglected despite the fact that the accreted matter should bring angular momentum to the white dwarf. It is important to see whether the above conclusion on the fate of a double white dwarf merger is unchanged when the effect of rotation is included.

Recently, Piersanti et al. (2003a) investigated the effect of rotation on the evolution of white dwarfs that accrete CO-rich matter. They claim that the combined effects of accretion and rotation induce expansion to make the surface zone gravitationally unbound and hence suppresses further accretion in the double white dwarf merger. They argue that the above effect makes the accretion rate smaller than the critical value for the occurrence of the off-center carbon ignition, and hence the white dwarf can grow up to the Chandrasekhar mass to become a SN Ia. Following this scenario Piersanti et al. (2003b) obtained an evolutionary model leading to a central carbon ignition with reduced accretion rates.

Contrary to their assumption, however, Paczyński (1991) and Popham & Narayan (1991) had shown that when the surface rotation rate is nearly critical, angular momentum is transported from the star back to the accretion disk (see also Fujimoto (1995)) and the star can continue to accrete matter as long as matter exists around the star. This indicates that we should let matter accrete onto the white dwarf keeping the surface rotation velocity nearly critical. In this paper, according to the results of Paczyński (1991) and Popham & Narayan (1991), we assume that even after the accreting star is spun up close to the Keplerian velocity at the surface, the star accretes matter at the initial rate while the surface velocity remains equal to the Keplerian velocity. With this assumption we have computed models of C-O white dwarfs

that rapidly accrete CO-rich matter. A similar assumption was adopted by Yoon et al. (2003) to investigate the evolution of helium accreting white dwarfs.

2. Models

The initial models, carbon-oxygen white dwarfs of $0.8M_{\odot}$ and $1M_{\odot}$, were obtained from zero-age helium main-sequence models by artificially suppressing nuclear reactions and converting chemical compositions to $(X_C, X_O, X_h) = (0.48, 0.50, 0.02)$ where X_h denotes the mass fraction of elements heavier than O, and by letting cool until the central temperature became $\sim 10^7$ K. Table 1 lists physical characteristics of the initial models. Adopted input physics are mostly the same as those used in Saio & Nomoto(1998): OPAL opacity tables (Iglesias & Rogers 1996), neutrino emission rates by Itoh et al. (1989), and carbon-burning reaction rates by Caughlan & Fowler (1988).

Keeping our evolutionary models spherical symmetric, we have included the effect of rotation only in the equation of hydrostatic equilibrium as

$$\frac{1}{\rho} \frac{dP}{dr} = -\frac{GM_r}{r^2} + \frac{2}{3}r\Omega^2, \quad (1)$$

where Ω is the angular velocity of rotation. The factor 2/3 comes from taking the mean of the radial component of the centrifugal force on a sphere (Kippenhahn et al. 1970). Spatial and time variation of Ω is determined by solving the conservation equation of angular momentum

$$\left[\frac{\partial(r^2\Omega)}{\partial t} \right]_{M_r} = \frac{\partial}{\partial M_r} \left[(4\pi\rho r^3)^2 \nu \frac{\partial\Omega}{\partial M_r} \right], \quad (2)$$

where ν stands for turbulent viscosity. The outer boundary condition $\Omega = \Omega_K$ was imposed at the photosphere, where $\Omega_K = \sqrt{GM/R^3}$ is the Keplerian angular velocity at the stellar radius R . We have neglected the rotation of the initial models.

We have adopted two kinds of formulae for the turbulent viscosity; one from Fujimoto (1993) and another from Zahn (1992). The turbulent viscosity formulated by Fujimoto (1993) includes the effect of baroclinic instability as well as shear instability. We will refer this case as case A; the viscosity is given by

$$\nu_A = \nu_{KH} + \nu_{BC}, \quad (3)$$

TABLE 1
PHYSICAL CHARACTERISTICS OF INITIAL MODELS

M/M_{\odot}	$\log T_c$	$\log \rho_c$	$\log L/L_{\odot}$	$\log R/R_{\odot}$
0.8	7.086	7.024	-2.286	-1.999
1.0	7.081	7.528	-2.216	-2.105

where

$$\nu_{\text{KH}} = \begin{cases} \frac{1}{2Ri^{1/2}}(1-4Ri)^{1/2}H_p^2N & \text{for } Ri < 1/4 \\ 0 & \text{for } Ri \geq 1/4; \end{cases} \quad (4)$$

$$\nu_{\text{BC}} = \begin{cases} \frac{1}{3Ri^{1/2}}H_p^2\Omega & \text{for } Ri \leq Ri_{\text{BC}} \\ \frac{1}{3Ri^{3/2}}H_p^2\Omega & \text{for } Ri > Ri_{\text{BC}}, \end{cases} \quad (5)$$

$$Ri = N^2 \left(\frac{d\Omega}{d \ln r} \right)^{-2}, \quad Ri_{\text{BC}} = 4 \left(\frac{r}{H_p} \right)^2 \frac{\Omega^2}{N^2} \quad (6)$$

with N being Brunt-Väisälä frequency defined as $N^2 = g(\Gamma_1^{-1} d \ln P / dr - d \ln \rho / dr)$ and H_p the pressure scale height.

For the second case, which is referred to as case B, we have included turbulent viscosity due to vertical shear instability formulated by Zahn (1992) but neglected the effect of meridional circulation; we have used the following equation,

$$\nu_B = \frac{2}{45} \frac{K}{N^2} \left(\frac{d\Omega}{d \ln r} \right)^2, \quad (7)$$

where K is the thermal diffusivity defined by $K = 4acT^3/(3\kappa\rho^2C_p)$. As we will see in the next section, the viscosity in case A is so efficient in transporting the angular momentum that the rotation becomes nearly uniform in the white-dwarf interior. In case B, on the other hand, the angular momentum is slowly transported into the deep interior. We assume that the two models for the transport of angular momentum bracket what occurs in a real star.

3. Numerical Results

Figure 1 shows the evolution of radius as a function of the total mass for C-O white-dwarfs that accrete CO-rich matter at rates of 10^{-5} and $5 \times 10^{-6} M_{\odot} \text{y}^{-1}$ from the beginning of accretion

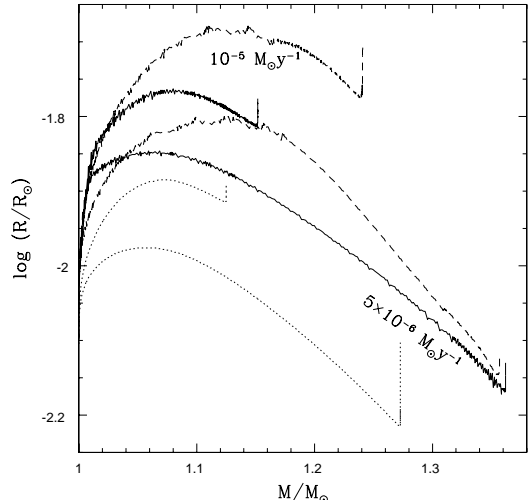


Fig. 1.— Evolution of C-O white dwarfs that accrete CO-rich matter at rates of 10^{-5} and $5 \times 10^{-6} M_{\odot} \text{y}^{-1}$. The solid (case A) and dashed (case B) lines are for rotating models in which the angular momentum transport is calculated using relatively high (A) and low (B) turbulent viscosity, respectively. The dotted lines are for non-rotating models. The nearly vertical increase in radius at the end of each evolution indicates the occurrence of an off-center carbon ignition.

to the off-center carbon ignition. The initial mass of the models is $1M_{\odot}$. Wiggles seen in this figure are numerical artifacts. The dotted lines show the evolution of non-rotating models, the solid lines for rotating models in case A, and the dashed lines for rotating models in case B. A nearly vertical increase in radius indicates the occurrence of the off-center carbon ignition. In the early phase of accretion the radius of the white dwarf increases because its envelope is heated by the accretion, and the centrifugal force of rotation lifts the envelope. In later phase of accretion, on the other hand, the radius begins to decrease as a result of increasing total white-dwarf mass. The lifting effect of rotation makes the radius of a rotating model larger than that of the non-rotating model with the same mass and the accretion rate. For a given accretion rate, the off-center carbon ignition occurs later in a rotating model than in the non-rotating model; i.e., the total mass at the carbon ignition is larger than that for the corresponding non-rotating model.

Figure 2 shows temperature versus M_r in the interior of models close to the off-center carbon ignition. These models have evolved from the initial model of $1M_{\odot}$ with an accretion rate of $10^{-5}M_{\odot}\text{y}^{-1}$. The solid and dashed lines are for rotating models, and the dotted line for a non-rotating model. The outer layers consisting of accreted matter ($M_r > 1M_{\odot}$) have high temperatures heated by the gravitational energy release. The heat is conducted into the layers of the original white dwarf. The heat-conduction front, however, has not advanced much during the time between the start of accretion and the off-center ignition ($\sim 10^4\text{y}$). Rotating models have broader temperature peaks than the non-rotating model, because they accrete more mass and hence the time from the start of accretion to the carbon ignition is longer. The core temperature has increased from the initial value $\log T = 7.08$ due to compression.

Table 2 lists the total mass M_{ig} and the central density ρ_c of the model in which the off-center carbon-ignition occurs, and the mass interior to the ignition layer $M_r(\text{ig})$ for each case computed, where the values of masses are given in units of M_{\odot} , \dot{M} means accretion rate in units of $M_{\odot}\text{y}^{-1}$, and M_i stands for the initial mass. The difference in M_{ig} between a rotating and the non-rotating model for a given accretion rate can be as large as

$\sim 0.1M_{\odot}$. The value of $M_r(\text{ig})$ is also larger in the rotating model. Rotation delays the carbon ignition because the centrifugal force reduces the effective gravity to lift the outer layers and reduce the temperature there (Piersanti et al. 2003a). The lifting effect of rotation appears also in the central density, ρ_c , which is lower in a rotating model than in a non-rotating model with a similar mass. Table 2 shows that the results hardly depend on the initial mass of the white dwarf.

The effects of rotation on M_{ig} and $M_r(\text{ig})$ for the case B models with $\dot{M} = 10^{-5}M_{\odot}\text{y}^{-1}$ are larger than those for the corresponding case A models. This is understood as follows: since, as discussed below, the angular momentum transport in case B is less efficient, angular momentum is accumulated around the ignition zone and the rotation speed there is faster and hence the effect of rotation is stronger than in the corresponding case A model in which Ω is nearly constant.

Figure 3 shows runs of the ratio of angular velocity to its local critical value, $\Omega/\Omega_{K,r}$, in the interior of models at evolutionary stages around carbon ignition. Here $\Omega_{K,r} = \sqrt{GM_r/r^3}$ is the local Keplerian velocity. Shown are the case A and case B models with accretion rates of $\dot{M} = 10^{-5}$, 5×10^{-6} and $3 \times 10^{-6}M_{\odot}\text{y}^{-1}$. In all cases, $\Omega/\Omega_{K,r}$ increases rapidly toward the surface in the very superficial layer, which is mainly due to a rapid increase in the radius of mass shell toward the surface. In case A the viscous transport of angular momentum is very efficient so that the rotation becomes nearly uniform (Fig. 4). Therefore, the dashed curves in Fig. 3 are almost parallel to the runs of $r^{3/2}M_r^{-1/2}$. In case B, on the other hand, the transport of angular momentum is not so efficient that the angular momentum is hardly transported into the original white dwarf ($M_r \leq 1M_{\odot}$). The peak in $\Omega/\Omega_{K,r}$ at $M_r \approx 1.05M_{\odot}$ for $\dot{M} = 10^{-5}M_{\odot}\text{y}^{-1}$ appears because the accreted matter is compressed with more or less conserving the angular momentum. Because of the fast rotation in the envelope, M_{ig} and $M_r(\text{ig})$ in case B with $\dot{M} = 10^{-5}M_{\odot}\text{y}^{-1}$ are larger than those for case A. For lower accretion rates, the distribution of $\Omega/\Omega_{K,r}$ is smoother and no peak exists, because the timescale of evolution is longer.

Figure 4 shows the runs of angular frequency of

TABLE 2
SUMMARY OF NUMERICAL RESULTS

\dot{M}	M_i	No rot.				Rot. A			Rot. B		
		$M_r(\text{ig})$	M_{ig}	$\log \rho_c$	$M_r(\text{ig})$	M_{ig}	$\log \rho_c$	$M_r(\text{ig})$	M_{ig}	$\log \rho_c$	
3×10^{-6}	1.0	1.35	1.36	9.15	1.38	1.40	9.09	1.38	1.40	9.26	
3×10^{-6}	0.8	1.35	1.36	9.13	1.39	1.40	9.07	1.38	1.40	9.25	
5×10^{-6}	1.0	1.24	1.27	8.47	1.33	1.36	8.63	1.32	1.35	8.70	
5×10^{-6}	0.8	1.25	1.28	8.48	1.34	1.37	8.64	1.32	1.36	8.69	
1×10^{-5}	1.0	1.05	1.12	7.82	1.07	1.15	7.83	1.12	1.24	7.94	
1×10^{-5}	0.8	0.98	1.09	7.65	1.01	1.13	7.70	1.06	1.15	7.76	

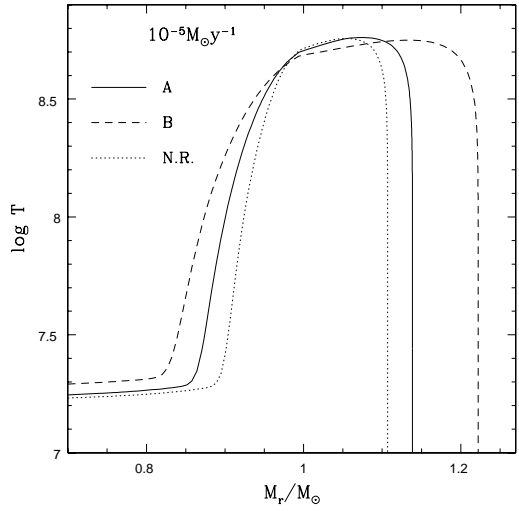


Fig. 2.— Temperature distributions in models close to the off-center carbon ignition for an accreting rate of $10^{-5} M_{\odot} \text{y}^{-1}$. The solid and the dashed line are for rotating models with different turbulent viscosities. The dotted line is for the non-rotating model.

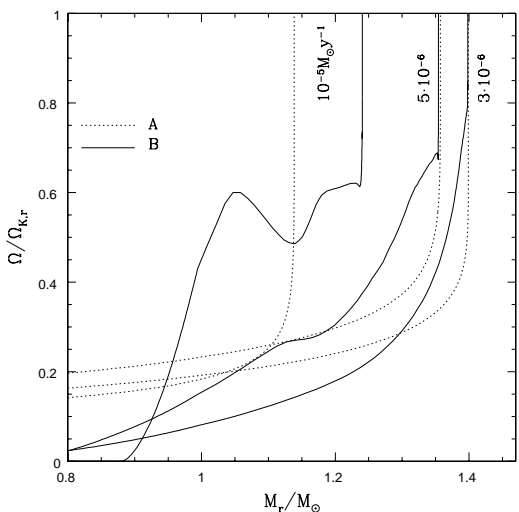


Fig. 3.— Runs of the ratio of angular frequency of rotation to the local Keplerian frequency, $\Omega_{K,r}$, in the interior of models for accretion rates of 10^{-5} , 5×10^{-6} , and $3 \times 10^{-6} M_{\odot} \text{y}^{-1}$. The abscissa represents the mass coordinate in units of solar mass.

rotation Ω in the interior of models at selected phases of evolution. Here the accretion rate is $\dot{M} = 3 \times 10^{-6} M_{\odot} \text{yr}^{-1}$ and the initial mass of the white dwarf is $1M_{\odot}$. Obviously, the angular momentum transport by the turbulent viscosity in case A is so efficient that $\Omega(M_r)$ is nearly constant in the interior (the dotted lines). In the very superficial layer, however, $\Omega(M_r)$ increases steeply toward the surface in the last model of case A. This stems from a rapid increase in the boundary value of $\Omega = \Omega_K \propto M^{1/2} R^{-3/2}$, i.e., Keplerian velocity at the stellar surface; this results from a rapid decrease in R as M is approaching to the critical white-dwarf mass. The surface rotation velocity increases so rapidly that the inward transport of angular momentum is not efficient enough to keep the angular velocity of rotation in the interior close to the surface value.

The angular momentum transport in case B is not so efficient as shown by the solid lines; the angular momentum is only gradually diffused into the original white dwarf interior ($M_r \leq 1M_{\odot}$). There is a peak in $\Omega(M_r)$ in the interior of the case B model. The peak value of Ω is higher than the surface value. Such a peak is produced by the compression of matter whose angular momentum is nearly conserved.

4. Conclusion

Taking into account the centrifugal force of rotation, we computed models of CO-white dwarfs that accrete CO-rich matter up to the carbon-ignition. We assumed that the surface angular velocity is equal to the Keplerian angular velocity. We have found that carbon is ignited in an outer layer if the accretion rate is greater than $3 \times 10^{-6} M_{\odot} \text{yr}^{-1}$. The rotation delays the ignition. The difference in the total mass at the ignition between rotating and non-rotating models can be as large as $\sim 0.1 M_{\odot}$, depending on the assumed turbulent viscosity and the accretion rate (see Uenishi, Nomoto, Hachisu (2003) for the 2D models).

Piersanti et al. (2003a,b) argued that when a sufficient angular momentum is accumulated in the accreting white dwarf, the surface becomes gravitationally unbound and then the accretion rate should be reduced to the rate at which the gravitational wave radiation carries away the angular momentum from the star. They have con-

cluded that no off-center carbon ignition but a SN Ia occurs in the merging double C-O white dwarfs. They ignored, however, the results of the investigations by Paczyński (1991) and Popham & Narayan (1991) who had shown that the angular momentum can be transported back to the accretion disk when the rotation speed is close to the critical one at the stellar surface so that the star can accrete as long as matter exists in the accretion disk. Our computations with assumptions in accordance with the results of Paczyński (1991) and Popham & Narayan (1991) yielded results contradicting the conclusions of Piersanti et al. (2003a,b).

When the double white dwarfs coalesce, the more massive white dwarf is expected to accrete CO-rich matter at a rate close to the Eddington limit ($\sim 10^{-5} M_{\odot} \text{yr}^{-1}$). We have found in this paper that such a high accretion rate leads to an off-center carbon ignition even if the effect of rapid rotation is included. Once the ignition occurs, the carbon flame propagates through the interior to the stellar center due to conduction and the C-O white dwarf is converted to an O-Ne-Mg white dwarf peacefully (Saio & Nomoto 1985, 1998; Timmes et al. 1994). The result of our computation including the effect of rotation confirms our previous conclusion that a double C-O white dwarf merger would *not* yield a SN Ia.

This work has been supported in part by the grant-in-Aid for Scientific Research (14047206, 14540223, 15204010) of the Ministry of Education, Culture, Sports, Science and Technology in Japan.

REFERENCES

- Benz, W., Cameron, A.G.W., Press, W.H., & Bowers, R.L., 1990, ApJ, 348, 647
- Caughlan, G.R. & Fowler, W.A. 1988, Atomic data Nuclear data tables 40, 283
- Fujimoto, M.Y. 1993, ApJ, 419, 768
- Fujimoto, M.Y. 1995, ApJ, 450, 262
- Iben, I.Jr., & Tutukov, A.V., 1984, ApJS, 54, 335
- Iglesias, C.A., & Rogers, F.J. 1996, ApJ, 464, 943

Itoh, N., Adachi, T., Nakagawa, M., Koyama, Y.,
Munakata, H., 1988, ApJ, 339, 354

Kawai, S., Saio, H., & Nomoto, K. 1987, ApJ, 315,
229

Kippenhahn, R., Meyer-Hofmeister, E., &
Thomas, H.C. 1970, å, 5, 155

Mochkovitch, R., Livio, M. 1990, A&A, 236, 378

Nomoto, K. 1984, ApJ, 277, 791

Nomoto, K. 1987, ApJ, 322, 206

Nomoto, K., & Iben, I., Jr. 1985, ApJ, 297, 531

Nomoto, K., & Kondo, Y. 1991, ApJ, 367, L19

Paczyński, B. 1991, ApJ, 370, 597

Piersanti, L., Gagliardi, S., Iben, I., Jr., & Tornambe, A. 2003a, ApJ, 583, 885

Piersanti, L., Gagliardi, S., Iben, I., Jr., & Tornambe, A. 2003b, ApJ, 598, 1229

Popham, R., & Narayan, P. 1991, ApJ, 370, 604

Rasio, F.A. & Shapiro, S.L., 1995, ApJ, 438, 887

Saio, H., & Nomoto, K. 1985, A&A, 150, L21

Saio, H., & Nomoto, K. 1998, ApJ, 500, 388

Timmes, F.X., Woosley, S.E., & Taam, R.E. 1994,
ApJ, 420, 348

Uenishi, T., Nomoto, K., & Hachisu, I. 2003, ApJ,
595, 1094

Webbink, R.F. 1984, ApJ, 277, 355

Yoon, S.-C., Langer, N., & Scheithauer, S. 2003,
preprint

Zahn, J.-P. 1992, A&A, 265, 115

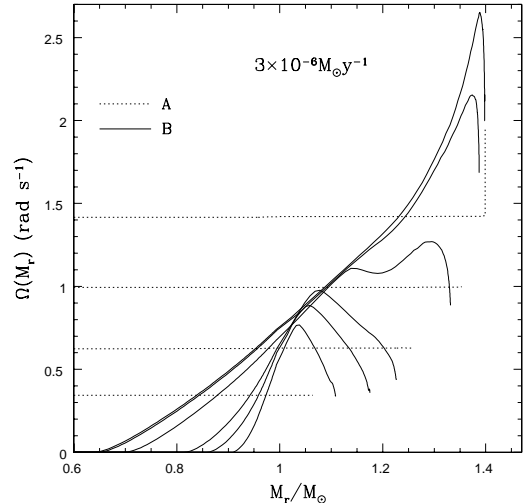


Fig. 4.— Runs of angular frequency of rotation, $\Omega(M_r)$, in the interior of models at selected evolutionary stages of accretion with a rate of $3 \times 10^{-6} M_\odot y^{-1}$.